Article

Cell Stem Cell

CD82/KAI1 Maintains the Dormancy of Long-Term Hematopoietic Stem Cells through Interaction with DARC-Expressing Macrophages

Graphical Abstract

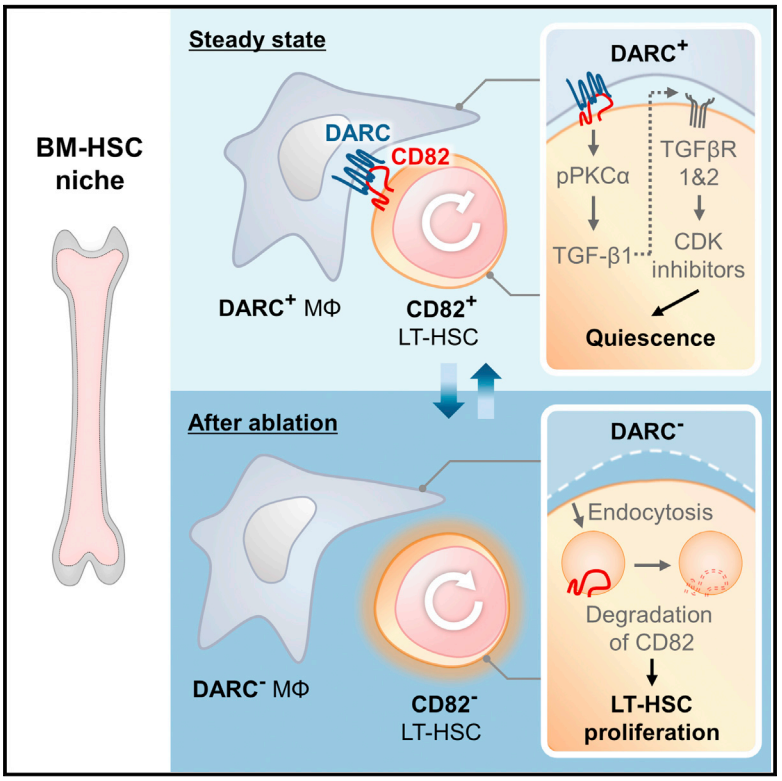

Highlights

- CD82/KAI1 is highly expressed on LT-HSCs in the bone marrow
- TGF-β1/Smad3 signaling downstream of CD82/KAI1 promotes LT-HSC quiescence
- CD82/KAI1 interacts with its binding partner, DARC, expressed on macrophages
- DARC binding maintains CD82/KAI1 on the HSPC surface and supports quiescence

Authors

Jin Hur, Jae-Il Choi, Hwan Lee, ..., Ho Lee, Sung Hee Baek, Hyo-Soo Kim

Correspondence

sbaek@snu.ac.kr (S.H.B.), hyosoo@snu.ac.kr (H.-S.K.)

In Brief

Hur et al. show that a conserved interaction between CD82/KAI1 on the surface of LT-HSCs and DARC on niche macrophages maintains LT-HSC quiescence through signaling-based inhibition of cell-cycle progression.

Accession Numbers

GSE56867

Hur et al., 2016, Cell Stem Cell *18*, 508–521
April 7, 2016
http://dx.doi.org/10.1016/j.stem.2016.01.013

CellPress

Cell Stem Cell
Article

CD82/KAI1 Maintains the Dormancy of Long-Term Hematopoietic Stem Cells through Interaction with DARC-Expressing Macrophages

Jin Hur,[1,2,9] Jae-Il Choi,[1,2,9] Hwan Lee,[1,2,9] Pniel Nham,[1,2] Tae-Won Kim,[1,2] Cheong-Whan Chae,[1,2] Ji-Yeon Yun,[1,2] Jin-A Kang,[1,2] Jeehoon Kang,[1] Sang Eun Lee,[1] Chang-Hwan Yoon,[3] Kyungjin Boo,[4] Seokjin Ham,[5] Tae-Young Roh,[5] Jong Kwan Jun,[6] Ho Lee,[7] Sung Hee Baek,[4,*] and Hyo-Soo Kim[1,2,8,*]

[1]National Research Laboratory for Stem Cell Niche, Center for Medical Innovation, Seoul National University Hospital, Seoul 110-744, Republic of Korea

[2]Innovative Research Institute for Cell Therapy, Seoul National University Hospital, Seoul 110-744, Republic of Korea

[3]Cardiovascular Center and Department of Internal Medicine, Seoul National University Bundang Hospital, Seongnam, Gyeonggi-do 463-707, Republic of Korea

[4]Creative Research Initiative Center for Chromatin Dynamics, School of Biological Sciences, Seoul National University, Seoul 151-742, Republic of Korea

[5]BK21PLUS Fellowship Program, Division of Integrative Biosciences and Biotechnology, Department of Life Sciences, Pohang University of Science and Technology (POSTECH), Pohang 790-784, Republic of Korea

[6]Department of Obstetrics and Gynecology, Seoul National University College of Medicine, Seoul 110-744, Republic of Korea

[7]Division of Convergence Technology, National Cancer Center, Gyeonggi-do 410-769, Republic of Korea

[8]Molecular Medicine and Biopharmaceutical Sciences, Graduate School of Convergence Science and Technology, Seoul National University, Seoul 110-744, Republic of Korea

[9]Co-first author

*Correspondence: sbaek@snu.ac.kr (S.H.B.), hyosoo@snu.ac.kr (H.-S.K.)

http://dx.doi.org/10.1016/j.stem.2016.01.013

SUMMARY

Hematopoiesis is regulated by crosstalk between long-term repopulating hematopoietic stem cells (LT-HSCs) and supporting niche cells in the bone marrow (BM). Here, we examine the role of CD82/KAI1 in niche-mediated LT-HSC maintenance. We found that CD82/KAI1 is expressed predominantly on LT-HSCs and rarely on other hematopoietic stem-progenitor cells (HSPCs). In *Cd82*$^{-/-}$ mice, LT-HSCs were selectively lost as they exited from quiescence and differentiated. Mechanistically, CD82-based TGF-β1/Smad3 signaling leads to induction of CDK inhibitors and cell-cycle inhibition. The CD82 binding partner DARC/CD234 is expressed on macrophages and stabilizes CD82 on LT-HSCs, promoting their quiescence. When DARC^{+} BM macrophages were ablated, the level of surface CD82 on LT-HSCs decreased, leading to cell-cycle entry, proliferation, and differentiation. A similar interaction appears to be relevant for human HSPCs. Thus, CD82 is a functional surface marker of LT-HSCs that maintains quiescence through interaction with DARC-expressing macrophages in the BM stem cell niche.

INTRODUCTION

Hematopoietic stem cell (HSC) transplantation is the most widely used regenerative therapy for a variety of life-threatening hematologic diseases. An essential factor for successful transplantation is the fine adjustment of hematopoiesis, determined by HSCs residing in specialized microenvironments, termed bone marrow (BM) niches (Morrison and Scadden, 2014). While most HSCs remain dormant in the BM stem cell niche, they undergo cycles of quiescence and self-renewal depending on blood cell requirements, which are controlled by cell-cycle regulators (Tesio and Trumpp, 2011; Zon, 2008). At the top of the hematopoietic hierarchy, long-term repopulating hematopoietic stem cells (LT-HSCs) have long-lasting self-renewal and differentiation capacity, which enables lifelong production of all hematopoietic lineages, whereas multipotent progenitor cells (MPPs) only possess transient differentiation capacity (Doulatov et al., 2012). Although several sets of cell-surface markers that distinguish HSCs from progenitor cells (e.g., MPPs) have been reported (Doulatov et al., 2012), the functional significance of these molecules remains elusive. In addition to signature molecules on LT-HSCs, other important factors that may influence the behavior of HSCs, particularly the quiescence-proliferation decision, include various environmental factors within the BM such as angiopoietin-1, osteopontin, stromal derived factor-1 (SDF-1), thrombopoietin, and hypoxia inducible factor-1 alpha (HIF-1α) (Kiel and Morrison, 2008; Takubo et al., 2010).

We reported that *Cd82*, also known as *Kangai1* (*Kai1*), possesses a hypoxia responsive element in its promoter region and that its expression is increased in ischemic tissues (Kim et al., 2010). CD82/KAI1 (CD82 hereafter) belongs to the tetraspanin superfamily and was initially identified in studies of T cell activation (Liu and Zhang, 2006; Miranti, 2009). In particular, CD82 has attracted attention because low CD82 expression has been associated with progression of solid tumors and

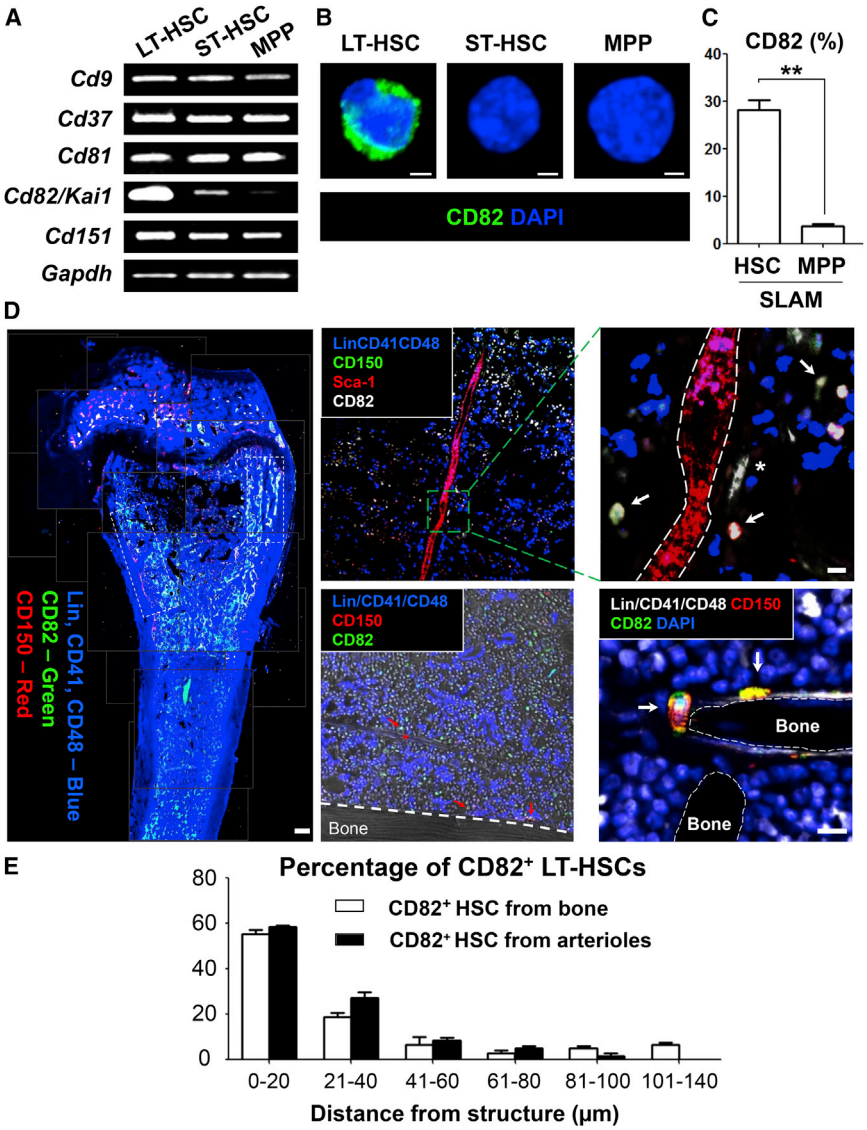

Figure 1. CD82 Is Expressed Predominantly on LT-HSCs in the BM Niche

(A) mRNA analysis of the tetraspanin family in BM LT-HSCs, ST-HSCs, and MPPs (n = 3, hereafter, n represents the number of biological replicates.)

(B) IF staining of CD82 expressed on BM LT-HSCs, ST-HSCs, and MPPs. Scale bar, 2 μm (n = 8).

(C) FACS analysis of the $CD82^+$ portion of BM SLAM-HSCs and SLAM-MPPs. BM HSPCs were isolated from the femur and tibia of a single hindlimb from WT mice (**$p < 0.05$, n = 3).

(D) (Left) The femoral bone was stained with lineage cocktail (blue), CD41 (blue), CD48 (blue), CD82 (green), and CD150 (red). White boxes indicate $CD82^+$ LT-HSC-enriched areas near the endosteal surface. Scale bar, 200 μm. (Top right) The arteriolar niche was stained with lineage cocktail (blue), CD41 (blue), CD48 (blue), CD82 (white), CD150 (green), and Sca-1 (red). The far-right panel shows a high-magnification image of the green boxed area from the left panel. Arrows indicate $CD82^+$ LT-HSCs in the BM niche. An asterisk indicates putative MSCs in the arteriolar niche. Scale bar, 20 μm. (Bottom right) The endosteal niche was stained with lineage cocktail (blue), CD41 (blue), CD48 (blue), CD82 (green), and CD150 (red). The high-magnification image on the far-right side shows the endosteal niche stained with lineage cocktail (white), CD41 (white), CD48 (white), CD82 (green), and CD150 (red). Arrows in both figures indicate $CD150^+CD82^+$ LT-HSCs. A red asterisk indicates the arteriolar niche. Scale bar, 20 μm.

(E) Distribution of the distances of $Lin^-CD48^-CD41^-CD150^+CD82^+$ HSCs from the endosteal and arteriolar niches in the femoral BM (~60% were within 20μm from both niches) (n = 4 mice, 7 sections, 162 individually validated cells). All error bars indicate SEM. See also Figure S1. For (D), the femoral bone image is a composite; individual images are indicated with gray lines. Unprocessed individual images are available in Data S1.

because it has been shown to suppress metastasis (Kim et al., 2005; Miranti, 2009). Moreover, CD82 is ubiquitously expressed and evolutionally conserved (Liu and Zhang, 2006), suggesting its functional significance in non-tumor cells as well.

Duffy antigen receptor for chemokines (DARC)/CD234 (DARC hereafter) is a seven-transmembrane domain protein expressed on erythrocytes, vascular endothelium, and a subset of epithelial cells (Peiper et al., 1995). Previous reports have shown that endothelial DARC induces senescence of $CD82^+$ tumor cells by directly binding to CD82 and is therefore thought to be essential for CD82-mediated suppression of cancer metastasis (Bandyopadhyay et al., 2006; Khanna et al., 2014). However, there are no published data regarding the surface expression of DARC on niche supporting cells (NSPs) or its role in the BM niche. In this study, we generated $Cd82^{-/-}$ mice and investigated the role of CD82 and DARC, along with cells expressing the each molecule, in the BM stem cell niche.

RESULTS

CD82 Is Expressed Predominantly on LT-HSCs

To examine association between the hypoxia-responsive gene *Cd82* and the BM stem cell niche, which is a hypoxic tissue, we analyzed the expression of CD82 and other tetraspanin members in highly purified mouse BM hematopoietic stem-progenitor cells (HSPCs; LT-HSCs, short-term repopulating hematopoietic stem cells [ST-HSCs], and MPPs) using defined sets of markers: LT-HSCs ($CD34^-Flt3^-Lineage^-Sca\text{-}1^+c\text{-}Kit^+$; LSK) and progeny, including ST-HSCs ($CD34^+Flt3^-$LSK) and MPPs ($CD34^+Flt3^+$LSK) (Figure S1A).

Interestingly, *Cd82* was expressed predominantly in LT-HSCs, but little was detected in ST-HSCs and MPPs at the mRNA level. In contrast, other members of the tetraspanin superfamily (*Cd9*, *Cd37*, *Cd81*, and *Cd151*) were expressed in every HSPC population (Figure 1A). Similar observations were made at the protein level by immunofluorescence (IF) (Figures 1B and S1B).

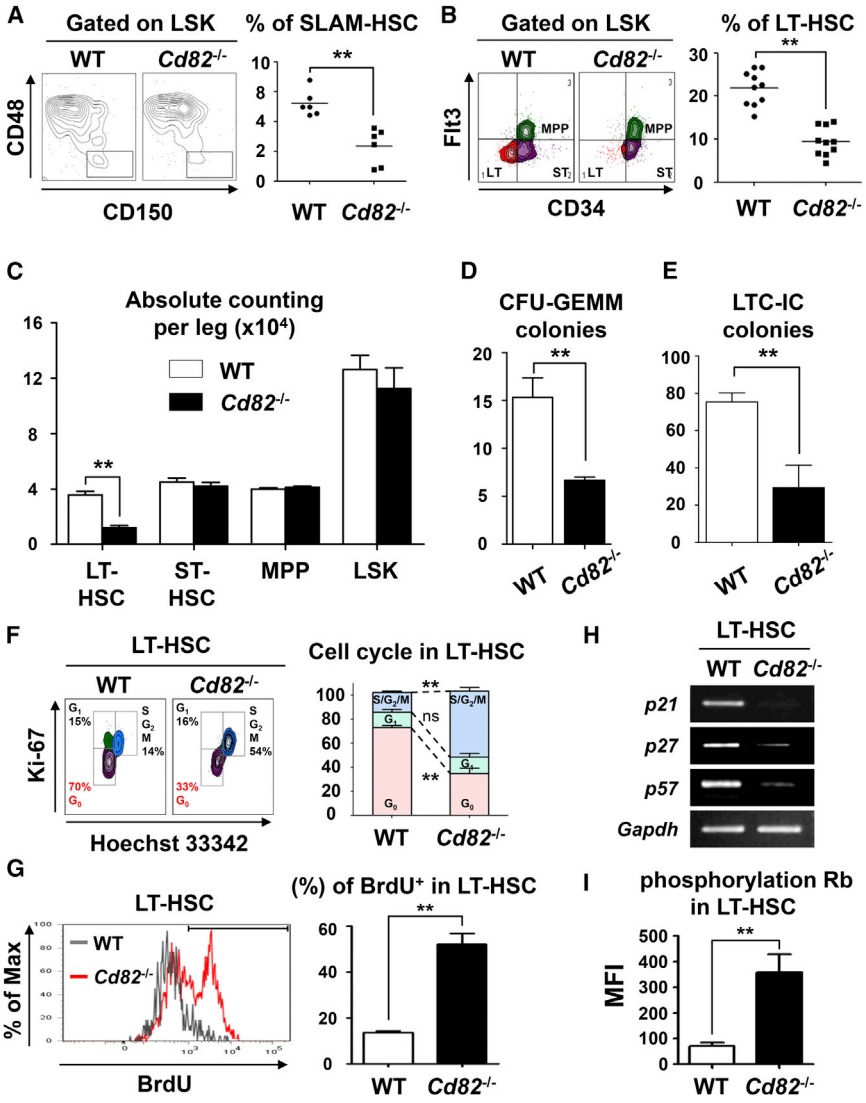

Figure 2. LT-HSCs Are Reduced and Exited from Quiescence in *Cd82*$^{-/-}$ Mice

(A) Percentage of SLAM-HSCs (CD48$^-$CD150$^+$) among BM LSK of WT and *Cd82*$^{-/-}$ mice (**p < 0.05, n = 6).

(B) (Left) FACS plot showing LT-HSCs (CD34$^-$Flt3$^-$), ST-HSCs (CD34$^+$Flt3$^-$), and MPPs (CD34$^+$Flt3$^+$) in the LSK gate. (Right) Portion of LT-HSCs among LSK (**p < 0.05, n = 10).

(C) Absolute counts of BM HSPCs in WT or *Cd82*$^{-/-}$ mice. BM HSPCs were isolated from the femur and tibia of a single hindlimb from WT mice (**p < 0.05, n = 4).

(D) Quantification of CFU-GEMM colonies formed by WT and *Cd82*$^{-/-}$ BM cells (**p < 0.05, n = 3).

(E) Number of LTC-IC colonies formed by WT and *Cd82*$^{-/-}$ BM cells (**p < 0.05, n = 3).

(F) (Left) Cell cycle status of WT or *Cd82*$^{-/-}$ LT-HSCs. (Right) Quantification of the left plots (**p < 0.05, n = 5).

(G) (Left) BrdU incorporation into WT and *Cd82*$^{-/-}$ LT-HSCs. (Right) Mean percentage of BrdU-positive cells (**p < 0.05, n = 3).

(H) mRNA expression of CDK inhibitors (*p21*, *p27*, and *p57*) in WT and *Cd82*$^{-/-}$ LT-HSCs.

(I) FACS analysis of phosphorylated Rb (pRb) in LT-HSCs (MFI, mean fluorescence intensity; **p < 0.05, n = 4).

All error bars indicate SEM. See also Figure S2 and Tables S1 and S2.

A recent paper (Oguro et al., 2013) suggested another HSPC classification based on signaling lymphocytic activation molecule (SLAM) family markers: (1) SLAM-HSC, or quiescent HSC, with CD150$^+$CD48$^-$CD229$^-$CD244$^-$LSK and (2) SLAM-MPP with CD150$^-$CD48$^-$CD229$^-$CD244$^-$LSK. Fluorescence-activated cell sorting (FACS) analysis revealed that 27% of SLAM-HSCs were CD82 positive, in contrast to merely 4% of SLAM-MPPs (Figures 1C and S1C). Emerging evidence shows that the BM endosteal and arteriolar niches are indispensable for maintaining HSC dormancy (Adams and Scadden, 2006; Morrison and Scadden, 2014; Silberstein and Lin, 2013). Consistent with these reports, whole-mount immunostaining revealed that the majority of CD82$^+$ LT-HSCs were associated with the endosteal and arteriolar niches (Figures 1D and 1E). Taken together, these data indicate that CD82 is a cell surface marker for LT-HSCs in the BM stem cell niche.

The Number of BM LT-HSCs Is Significantly Reduced in *Cd82*$^{-/-}$ Mice

To examine whether CD82 affects biological behaviors of LT-HSCs, we generated the *Cd82*$^{-/-}$ mouse (Figures S2A and S2B). We double-confirmed the absence of CD82 on LT-HSCs and SLAM-HSCs derived from the BM of *Cd82*$^{-/-}$ mice (Figure S2C). The percentage of SLAM-HSCs (CD150$^+$CD48$^-$LSK cells) (Kiel et al., 2005) was significantly lower in the BM of *Cd82*$^{-/-}$ mice than in wild-type (WT) counterparts (Figure 2A). Next, we compared the number of LT-HSCs, ST-HSCs, and MPPs (Doulatov et al., 2012) in WT and *Cd82*$^{-/-}$ BM. The number of BM LT-HSCs was significantly lower in *Cd82*$^{-/-}$ mice than WT mice, whereas the number of ST-HSCs, MPPs, or LSKs was similar (Figures 2B and 2C). The number of total BM nucleated cells, complete blood counts, (Figure S2D; Table S1), total and each type of myeloid progenitor cells (Sca-1$^-$c-Kit$^+$ HSPCs in the Lin$^-$ gate) (common myeloid progenitor [CMP], granulocyte macrophage [Mφ] progenitor [GMP], and megakaryocyte erythroid progenitor [MEP]) were similar between the two groups (Figures S2E and S2F).

To further quantify the number of BM HSPCs and long-term repopulating cells, we performed an in vitro colony-forming unit (CFU) and long-term culture-initiating cell (LTC-IC) assay (Arai et al., 2004) using WT or *Cd82*$^{-/-}$ mice. *Cd82* deficiency significantly decreased the number of CFU-granulocyte, erythroid, monocyte, and megakaryocyte (CFU-GEMM) colonies as compared with WT (Figure 2D). Also, the number of LTC-ICs from the *Cd82*$^{-/-}$ BM was significantly lower than that from WT BM (Figure 2E). These data suggest that *Cd82*$^{-/-}$ mice show a selective decrease in LT-HSCs but that the numbers of ST-HSCs or MPPs are not affected.

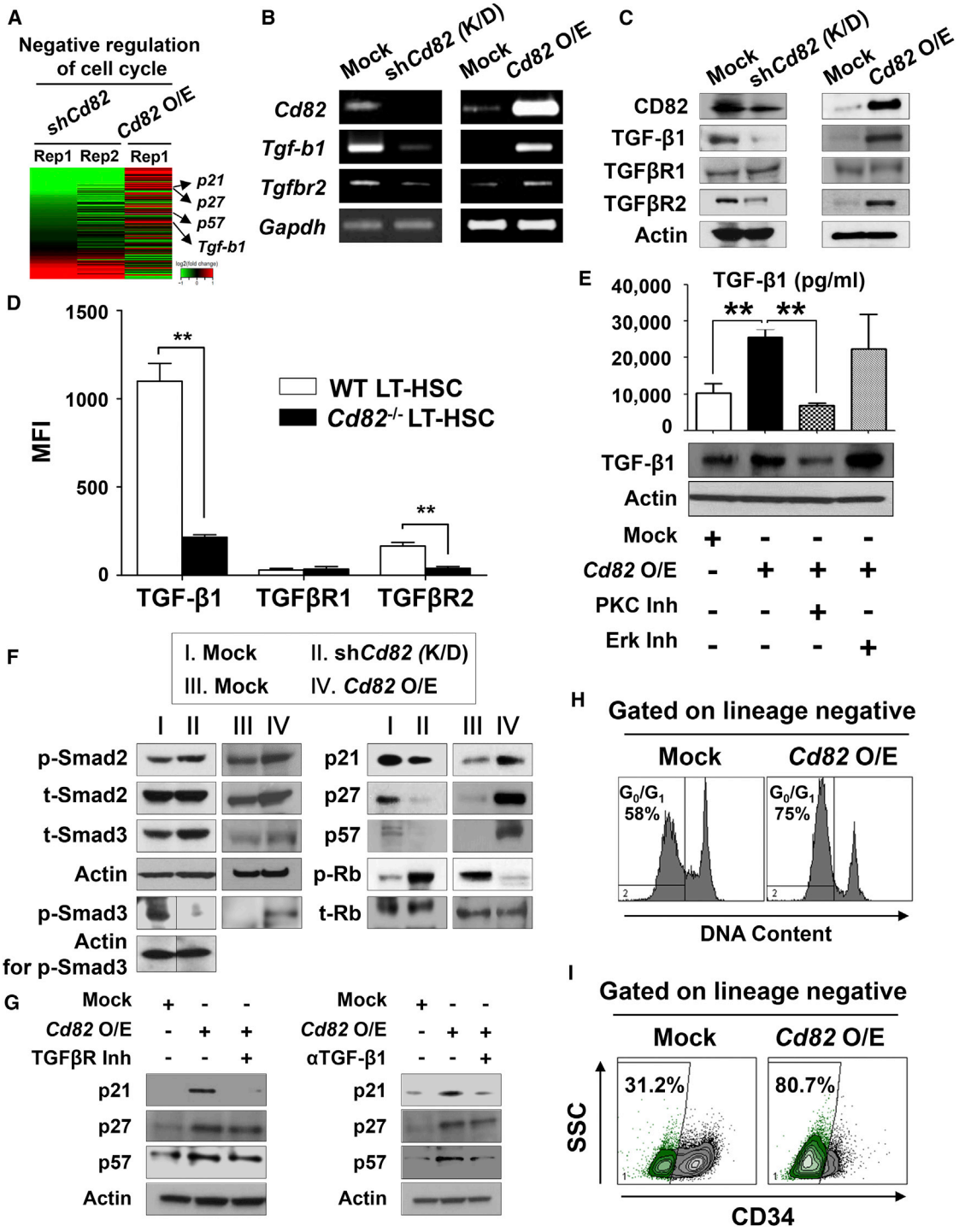

Figure 3. CD82 Activates TGF-β1 and TGFβR2 via PKCα and Induces Cell-Cycle Arrest of HSCs

(A) RNA-sequencing of *Cd82* K/D and O/E EML cells (n = 2 for *Cd82* K/D group, n = 1 for O/E group) (GO: 0045786).

(B) mRNA levels of *Cd82*, *Tgf-b1*, and *Tgfbr2* in *Cd82* K/D and *Cd82* O/E EML cells (n = 3).

(C) Western blot analysis of CD82, TGF-β1, TGFβR1, and TGFβR2 in *Cd82* K/D and *Cd82* O/E EML cells (n = 3).

(D) FACS analysis of TGF-β1, TGFβR1, and TGFβR2 expression on LT-HSCs from WT and *Cd82*$^{-/-}$ mice (**$p < 0.05$, n = 3)

(E) (Top) Multiplex ELISA of TGF-β1 secretion (n = 3, **$p < 0.05$). (Bottom) Western blot analysis of TGF-β1 expression in mock and *Cd82* O/E EML cells. To examine the involvement of PKC and Erk in the CD82-induced quiescence pathway, inhibitors for each molecule were used individually in the last two groups.

(F) Western blot analysis of Smad2, Smad3, CDK inhibitors, and Rb in mock, *Cd82* K/D, and *Cd82* O/E EML cells. In the *Cd82* K/D experimental set, Actin control (line 6) for the p-Smad3 blot (line 5) is presented right below the p-Smad3 blot. A divider was put between the lanes in the two blots to indicate that we cropped a lane (*Cd82* K/D clone 2) and merged the mock and *Cd82* K/D clone 3 lanes (only clone 3 was used in our analyses).

(legend continued on next page)

Cd82 Deficiency Leads to Loss of LT-HSC Quiescence

To determine why *Cd82*$^{-/-}$ mice had fewer BM LT-HSCs, we compared the cell-cycle status of BM LT-HSCs of WT and *Cd82*$^{-/-}$ mice. *Cd82* deficiency resulted in prominent cell-cycle progression, as reflected by a significantly lower percentage of LT-HSCs in G_0 as well as a marked increase in $S/G_2/M$ phase cells (Figures 2F and S2G).

To compare the in vivo proliferation of BM LT-HSCs of WT and *Cd82*$^{-/-}$ mice, we performed an in vivo bromodeoxyuridine (BrdU) incorporation assay. The rate of BrdU incorporation in LT-HSCs was significantly greater in *Cd82*$^{-/-}$ mice than WT (Figure 2G). Notably, we observed a reduction in cyclin dependent kinase (CDK) inhibitors in *Cd82*$^{-/-}$ LT-HSCs (Figure 2H). These findings were consistent with increased Rb phosphorylation, which induces cell-cycle entry (Tesio and Trumpp, 2011; Zou et al., 2011) (Figure 2I). These data suggest that *Cd82*$^{-/-}$ LT-HSCs are less quiescent and more proliferative than WT LT-HSCs.

CD82-Activated Signaling Promotes Cell-Cycle Arrest in LT-HSCs

To investigate the mechanisms by which CD82 maintains LT-HSC quiescence, we performed a series of in vitro gain- and loss-of-function experiments using EML (erythroid, myeloid, and lymphocytic: a mouse BM-derived hematopoietic precursor cell line), which is considered an ideal surrogate for primary HSPCs and has been widely used in HSC studies (Ye et al., 2005; Zou et al., 2011). We examined CD82 expression in two different EML populations: the quiescent Lin$^-$CD34$^-$ fraction and the actively cycling Lin$^-$CD34$^+$ population (Zou et al., 2011). Importantly, we observed prominent expression of CD82, both at the mRNA and protein levels, in the Lin$^-$CD34$^-$ fraction but little in the Lin$^-$CD34$^+$ population (Figures S3A and S3B). To perform gain- or loss-of-function assays, we established *Cd82* knockdown (K/D) and *Cd82* overexpressing (O/E) stable EML cell lines (Figures S3C and S3D).

Using RNA-sequencing (RNA-seq) analysis, we confirmed that CDK inhibitors were downregulated in *Cd82* K/D EML cells and upregulated in *Cd82* O/E EML cells (Figure 3A). Interestingly, TGF-β signal components that are upstream regulators of CDK inhibitors also changed upon *Cd82* O/E and K/D (Figures 3A and S3E).

Cd82 K/D in EML cells lowered TGF-β1 and TGFβR2 expression, while *Cd82* O/E increased their expression; TGFβR1 was not affected (Figures 3B and 3C). Excitingly, similar results were observed in FACS analysis of BM LT-HSCs of WT and *Cd82*$^{-/-}$ mice (Figure 3D). To investigate the functional link between CD82 and TGF-β1, we evaluated the PKCα and Erk pathways, which are known to be upstream regulators of TGF-β1 (Grewal et al., 1999; Shen et al., 2008). CD82 significantly induced both expression and secretion of TGF-β1, which were attenuated only by a PKC inhibitor, but not by an Erk inhibitor (Figure 3E).

Since CDK inhibitors were reported as downstream targets of the TGF-β/Smad3 pathway (Li et al., 1995; Scandura et al., 2004), we examined the activation of Smad2/3. *Cd82* O/E induced phosphorylation of Smad3, increased CDK inhibitors, and inhibited Rb phosphorylation, whereas the *Cd82* K/D gave opposite results (Figure 3F). Induction of CDK inhibitors by CD82 was blocked by a TGFβR inhibitor and TGF-β1 neutralization (Figure 3G). Interestingly, *Cd82* O/E repressed cell-cycle progression from the G_0/G_1 to S phase (Figure 3H) and increased the proportion of Lin$^-$CD34$^-$ quiescent EML (qEML) cells (Figure 3I).

Taken together, our results indicate that CD82 represses the cell cycle and maintains quiescence of LT-HSCs through the activation of TGF-β1/Smad3 signaling via PKCα, leading to induction of CDK inhibitors and cell-cycle arrest.

CD82 Regulates the Cell-Cycle Status and Long-Term Repopulation Capacity of LT-HSCs

We compared the BM recovery rate of WT and *Cd82*$^{-/-}$ mice after irradiation. *Cd82*$^{-/-}$ BM exhibited a greater ablation (Figure S4A), presumably because *Cd82* deficiency led to increased cell proliferation and resultant susceptibility to irradiation. To investigate whether CD82 affects the long-term repopulating capacity of HSCs, we performed a competitive BM transplantation (BMT) in which sublethally irradiated recipient mice (CD45.1) were transplanted with HSPC-enriched Lin$^-$ BM cells (CD45.2) from WT or *Cd82*$^{-/-}$ mice plus competitor cells (CD45.1) (Figure 4A). On week 16 post-BMT, we assessed the chimerism of donor-derived cells (CD45.2) in the recipient mice (CD45.1). The repopulating ability of *Cd82*$^{-/-}$ HSPCs was inferior to that of WT cells (Figure 4A). In the secondary BMT, the BM of mice that received *Cd82*$^{-/-}$ HSPCs had fewer LSKs and LT-HSCs than WT BM (Figure 4B). The percentage and number of LT-HSCs in G_0 was significantly greater in recipients receiving WT HSPCs (Figures 4C and 4D).

Notably, as much as 67% of *Cd82*$^{-/-}$ LT-HSCs were in G_1 phase (Figure 4C), which was quite different pattern than that shown in Figure 2F (in which only 16% were in G_1 and 54% in $S/G_2/M$ phase). Figure 2F shows an analysis of *Cd82*$^{-/-}$ LT-HSCs obtained from *Cd82*$^{-/-}$ whole-body-knockout mice, whereas Figure 4C shows the cell-cycle status of *Cd82*$^{-/-}$ donor-derived LT-HSCs harvested from WT recipient mice. Thus, we speculated such differences might be attributable to different CD82 expression of NSPs. Among BM niche components (osteoblasts [OBs], endothelial cells [ECs], and mesenchymal stromal cells [MSCs]), MSCs exhibited much greater CD82 expression versus ECs and OBs (Figures S4B–S4D).

To study the influence of MSCs on cell-cycle progression in LT-HSCs, we generated a *Cd82* K/D mesenchymal stromal cell line (C3H/10T1/2, hereafter 10T1/2) (Konieczny and Emerson, 1984) and co-cultured LT-HSCs isolated from *Cd82*$^{-/-}$ mice with mock or *Cd82* K/D 10T1/2 cells. LT-HSCs co-cultured with *Cd82* K/D MSCs exhibited higher $S/G_2/M$, lower G_1, and

(G) Protein levels of CDK inhibitors in mock, *Cd82* O/E EML cells, and *Cd82* O/E EML cells treated with TGFβR inhibitor, SB431542 (50 μM), or TGF-β1 neutralizing antibody.

(H) Percentage of G_0/G_1 phase cells among mock or *Cd82* O/E Lin$^-$ EML cells.

(I) FACS analysis of the Lin$^-$CD34$^-$ population from mock and *Cd82* O/E EML cells.

All error bars indicate SEM. See also Figure S3 and Table S2.

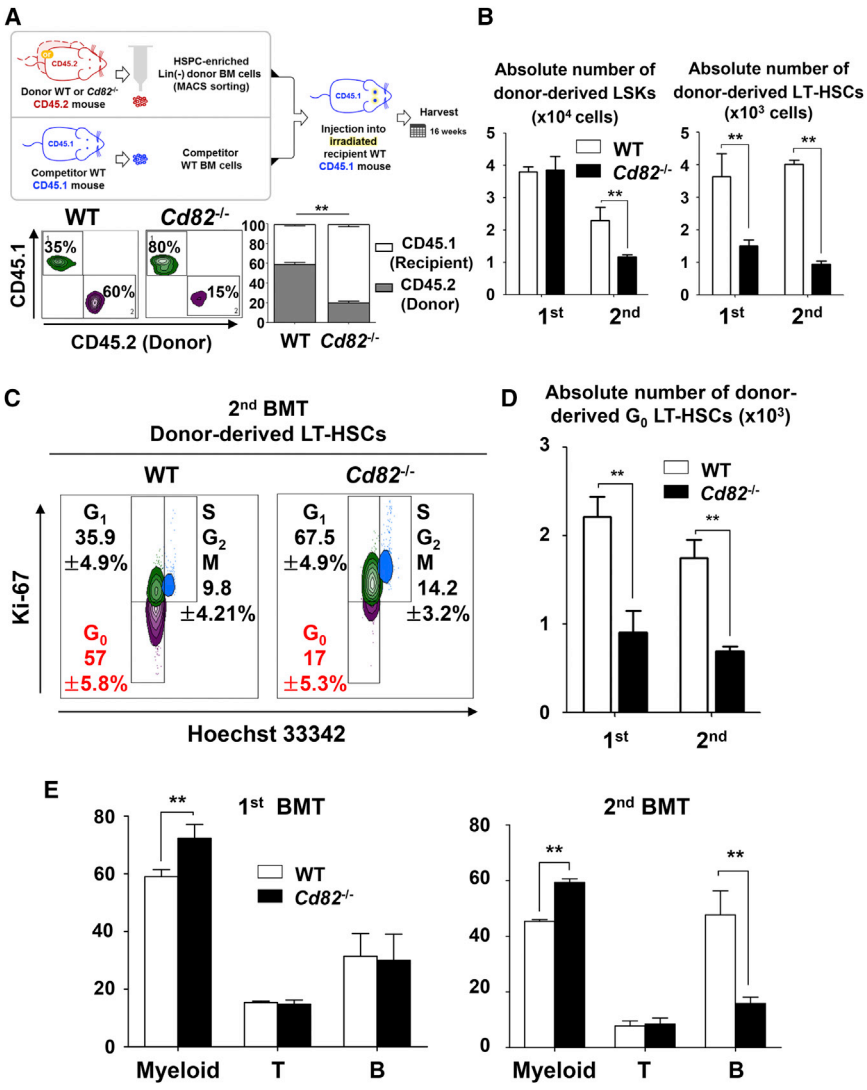

Figure 4. Role of CD82 in Post-transplant BM Repopulation

(A) (Top) Schematic representation of the competitive BMT. Donor (CD45.2)-derived Lin^- BM cells (WT or *Cd82*$^{-/-}$) and competitor cells (CD45.1) were transplanted in sublethally irradiated recipient mice (CD45.1). (Bottom) Mean percentage of donor- or recipient-derived cells in the peripheral blood 16 weeks after competitive BMT (**$p < 0.05$, $n = 3$).

(B) The repopulating capacity of WT and *Cd82*$^{-/-}$ cells was determined via quantification of the absolute numbers of donor-derived LSK (Left) and LT-HSCs (right) from recipient BM after primary or secondary BMT. All cell counts in Figure 4 were conducted with BM cells from the femur and tibia of a single hindlimb from WT mice. (**$p < 0.05$, $n = 3$).

(C) Cell-cycle status of donor-derived LT-HSCs after secondary BMT ($n = 3$).

(D) Absolute number of donor-derived LT-HSCs in G_0 after primary or secondary BMT (**$p < 0.05$, $n = 3$).

(E) The percentage of $CD11b^+$ myeloid cells (myeloid), $CD3^+$ T cells (T), or $CD45R/B220^+$ B cells (B) that were differentiated from donor-derived HSPCs after primary or secondary BMT (**$p < 0.05$, $n = 3$).

All error bars indicate SEM. See also Figure S4.

similar G_0 populations than LT-HSCs cultured with mock MSCs (Figure S4E), suggesting that CD82 on MSCs is important for G_1 check of LT-HSCs. *Cd82* K/D reduced *Tgf-b1* expression in 10T1/2 cells (Figure S4E), which may be the mechanism by which MSCs downregulate the G_1-to-S/G_2/M transition.

Another interesting observation from the serial BMT was that HSCs from *Cd82*$^{-/-}$ mice showed preferential differentiation toward a myeloid lineage (Figure 4E). These tendencies were also observed in fresh BM from WT and *Cd82*$^{-/-}$ mice (Figure S4F) and were corroborated by RNA-seq analysis of EML cells in which *Cd82* K/D decreased gene expression of negative regulators for myeloid differentiation (Figure S4F). We speculated such myeloid bias might be associated with CD82 expression on myeloid progenitors. However, myeloid progenitors displayed low CD82 expression: CMP (6.8% ± 2.3%), GMP (2.3% ± 1.4%), and MEP (1.2% ± 0.5%) (Figure S4B).

Collectively, these data indicate that CD82 plays a significant role in maintaining the long-term repopulating capacity of HSCs and that *Cd82*-deficient HSCs show myeloid-biased differentiation.

The CD82 Binding Partner DARC Is Highly Expressed on BM Niche Macrophages

The above findings led us to investigate the molecule that interacts with CD82 to activate the CD82-PKCα pathway in LT-HSCs. A previous report demonstrated that CD82 binds to DARC (Bandyopadhyay et al., 2006). Also, cells such as ECs, MSCs, OBs, and Mφ have all been shown to support the BM stem cell niche (Kiel and Morrison, 2008; Morrison and Scadden, 2014). Therefore, we examined whether and if so which of these cells express DARC. Interestingly, 38.4% ± 1.2% of BM Mφ ($CD11b^+Gr1^{low}F4/80^+SSC^{low}$) and as many as 64% ± 5% of $F4/80^+$ BM Mφ were $DARC^{high}$ (Figures 5A and S5B). Other niche-supporting cells (OBs, ECs, and MSCs) rarely expressed DARC (Figures S5A and S5C). $F4/80^+DARC^+$ Mφ was detected both in the arteriolar and endosteal niches (Figure 5B). Furthermore, 10% of $DARC^+$ Mφ expressed α-smooth muscle actin (α-SMA) and cyclooxygenase-2 (COX-2), which implies a functional overlap with a subset of Mφ that was recently been described to promote LT-HSC quiescence (Ludin et al., 2012) (Figure S5D). We also detected $DARC^+αSMA^+$ Mφ in the BM endosteal niche by IF analysis (Figure S5E). Therefore, we focused on investigating how DARC-expressing Mφ function through the molecule.

Next, we examined whether DARC on Mφ directly interacts with CD82 on LT-HSCs in the BM niche. IF staining of mouse bone revealed that $DARC^+$ Mφ are in direct contact with $CD150^+CD82^+$ quiescent LT-HSCs in the endosteal and arteriolar niches (Figure 5C). Since Tie2 has also been identified as

a marker for LT-HSCs (Arai et al., 2004), we employed Tie2-GFP mice. As expected, DARC was shown to have direct contact with CD82 on green LT-HSCs in the BM of Tie2-GFP mice (Figure 5C). In in vitro co-culture experiments, DARC on Mφ was adjacent to CD82 on HSPCs (Figure 5D) and $CD82^+$ HSPCs that were maintained with Mφ were less proliferative (Ki-67 negative) than mono-cultured $CD82^+$ HSPCs (Figure S5F). Direct interaction of CD82/DARC was also confirmed by co-immunoprecipitation of EML cell lysates (Figure 5E). Importantly, co-culture of primarily isolated HSPCs and Mφ induced G_0 arrest of LT-HSCs (Figure 5F).

In order to see whether DARC is involved in the anti-proliferative effect of Mφ, we analyzed the cell-cycle status of primary LT-HSCs after co-culture either with primary $DARC^+$ or with $DARC^-$ Mφ. As expected, while $DARC^+$ Mφ/HSPC co-culture successfully maintained dormancy of LT-HSCs, co-culture with $DARC^-$ Mφ did not (Figure S5G). The number of $CD82^+$ LT-HSCs that were cultured with $DARC^+$ Mφ was significantly higher than those cultured with $DARC^-$ Mφ (Figure S5H), given that the former were maintained as LT-HSCs while the latter underwent proliferation.

Next, we performed an in vitro mechanistic analysis using primary cells that were genetically manipulated with exogenous small hairpin RNA (shRNA) against *Tgf-b1* or *Smad3* (Figure S5I). HSPC/Mφ co-culture resulted in a 2-fold higher G_0 population in LT-HSCs versus HSPC mono-culture. Also, as expected, K/D of *Tgf-b1* or *Smad3* in LT-HSCs led to a decreased G_0 population even in the presence of $DARC^+$ Mφ. Additionally, HSPC/Mφ co-culture led to lower levels of Rb phosphorylation (i.e., cell-cycle downregulation) in mock-transduced LT-HSCs, but this response was compensated for by *Tgf-b1* or *Smad3* K/D in LT-HSCs (Figure 5G). These data indicate that DARC on Mφ triggers quiescence signaling in LT-HSCs via surface CD82 of LT-HSCs.

In contrast to broad expression of DARC on human ECs (Bandyopadhyay et al., 2006), only ~0–1% of the two types of mouse BM ECs were positive for DARC. Moreover, regardless of originating tissue, ECs very weakly expressed DARC (Figures S5A, S5J, and S5K). To determine the possible influence of endothelial DARC on cell-cycle status of LT-HSCs, we performed gain-of-function assays using two different endothelial cell lines (C166, MS-1) that were genetically manipulated to overexpress DARC (Figure S5L). Interestingly, there was virtually no difference in the cell-cycle status of LT-HSCs co-cultured either with mock or *Darc* O/E C166 cell lines (expressing high basal level of DARC), while the percent of LT-HSCs in G_0 that were co-cultured with *Darc* O/E MS-1 was significantly higher than those cultured with mock MS-1 cell line (expressing low basal level of DARC) (Figures S5L and S5M).

Thus, DARC, which is highly expressed on Mφ but rarely on ECs, regulates LT-HSC quiescence through direct contact with CD82 on LT-HSCs in the BM niche.

Ablation of DARC-Expressing Macrophages Reduces Surface CD82 Expression on LT-HSCs

To examine the role of CD82 and DARC in maintaining LT-HSC quiescence and reconstituting the BM after ablative intervention, we monitored sequential changes in $CD82^+$ LT-HSCs and proliferating blood cells after a single-dose of 5-FU. Since 5-FU induces apoptosis primarily in actively cycling progenitors and mature blood cells (Brenet et al., 2013; Winkler et al., 2012), the number of total BM cells rapidly decreased (Figure 6A), necessitating a new cell supply from quiescent LT-HSCs that survived the 5-FU treatment. In response to a reduction in BM cells, the percentage of $CD82^+$ cells in the $CD34^-$LSK population rose until day 2, plummeted to reach a nadir on day 5, and returned to a normal level ~2 weeks after 5-FU treatment (Figures 6B and S6A). Reduction in CD82 expression on LT-HSCs on day 5 was accompanied by the start of cell proliferation (Figures 6C and S6B).

In the BM myeloablation model, overall DARC expression was maintained till day 2 post 5-FU injection, dropped on day 5, and then recovered afterward (Figure S6C). The percent of $DARC^+$ Mφ elevated during the first 2 days after 5-FU challenge, decreased until 5-FU treatment day 5, and then gradually recovered (Figures 6D, 6E, and S6D). Importantly, according to our FACS analysis, Mφ is the only nucleated cell type that expresses DARC in the BM (Figure S5A). These data indicate that the recovery of DARC expression after BM ablation is due to an increase in $DARC^+$ Mφ.

The fact that CD82 and DARC directly contact each other, and that $CD82^+$ LT-HSCs and $DARC^+$ Mφ exhibit a similar pattern of rise and fall after 5-FU treatment (Figures 6B and 6D), led us to hypothesize that depletion of $DARC^+$ Mφ weakens CD82/DARC interactions, resulting in decreased CD82 levels on LT-HSCs. We tracked time-dependent changes in LT-HSC/Mφ interactions following 5-FU treatment. Bones that were harvested on day 5 post 5-FU injection showed only a few LT-HSCs and $DARC^+$ Mφ (Figure S6E). Importantly, neither LT-HSCs nor co-localization of LT-HSCs and $DARC^+$ Mφ was observed. On day 10 post-5-FU injection, bones clearly showed BM reconstitution. Interestingly, near the endosteal surface, several $DARC^+$ cells were clustered around LT-HSCs (Figure S6E).

Next, we investigated the effect of Mφ depletion by clodronate (Petersen et al., 2014) on $CD82^+$ LT-HSCs. Clodronate effectively removed total and $DARC^+$ Mφ (Figures S6F and S6G), leading to a marked reduction in the number of total and $CD82^+$ LT-HSCs (Figures 6F and S6H).

Next, we mimicked in vivo BM ablation by co-culturing qEML cells with various numbers of Raw 264.7 cells (mouse macrophage cell line). Of interest, CD82 expression was maintained on qEML co-cultured with Raw 264.7 cells, and CD82 levels on qEML were positively correlated with the number of co-cultured Raw 264.7 cells (Figure 6G).

To explore the direct influence of macrophagic DARC to regulate CD82 expression on HSC, we established a *Darc* K/D Raw 264.7 cell line (Figure S6I). CD82 on qEML cells significantly decreased when co-cultured with *Darc* K/D Raw 264.7 cells (Figure 6H).

We further investigated the mechanism through which CD82 is decreased. It has been reported that CD82 expression level is modulated by ubiquitination (Tsai et al., 2007) and endocytosis (Xu et al., 2009). Thus, we speculated that after losing direct contact with DARC on a macrophage, CD82 on LT-HSCs might first be ubiquitinated and then endocytosed. We detected CD82 ubiquitination when qEML cells were cultured in proliferation conditions (Figure 6I). Also, $CD82^+$ qEML cells maintained under

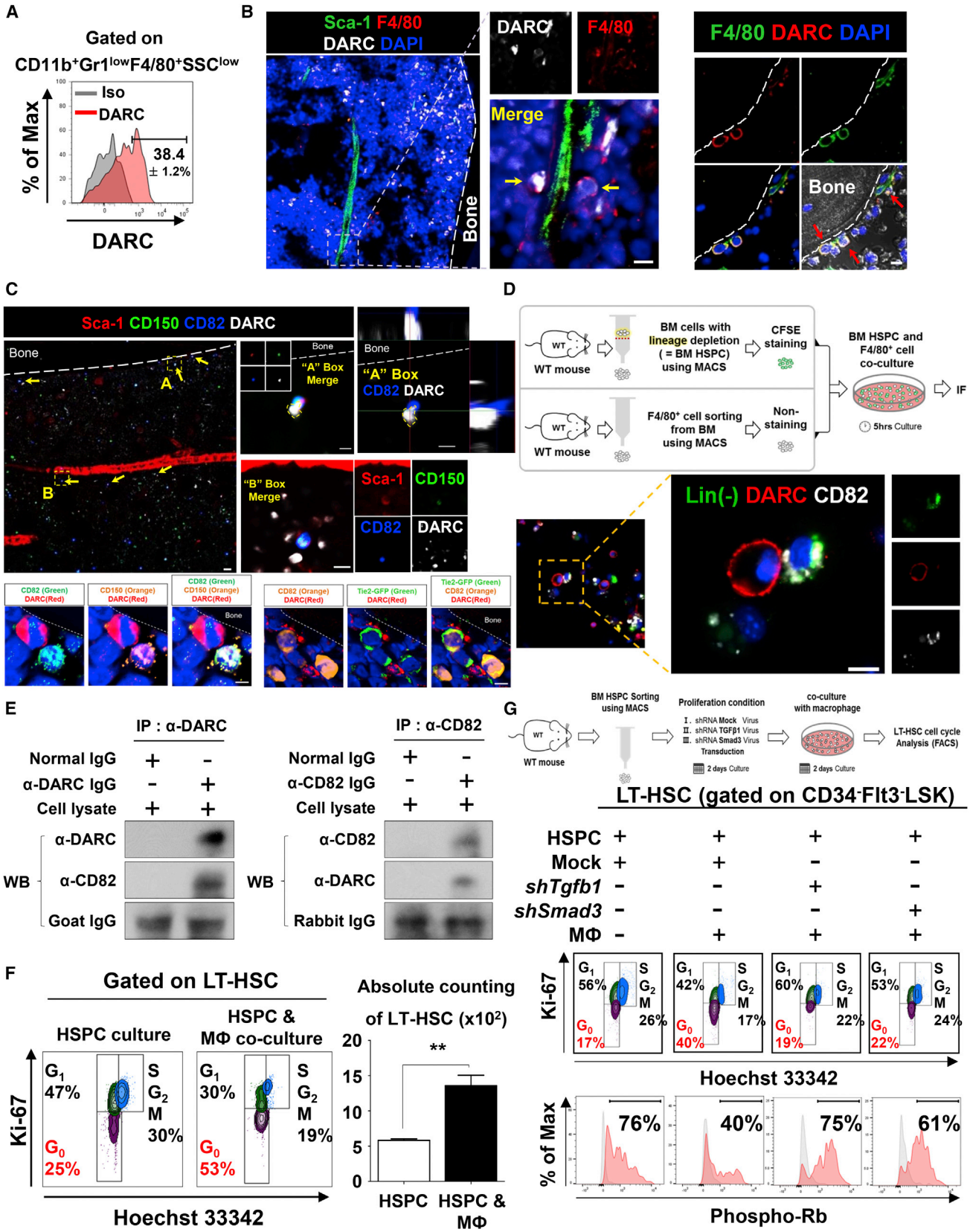

(legend on next page)

proliferation conditions for 2 days exhibited markedly reduced CD82 expression. Notably, CD82 expression on qEML cells was preserved by treatment with the proteasome inhibitor MG-132, similar to DARC$^+$ Mφ co-culture (Figure S6J).

Next, we performed an endocytosis assay on co-cultured qEML and Raw 264.7 cells. When co-cultured with DARC-positive "mock" Mφ, qEML showed no sign of CD82 endocytosis. However, when qEML cells were cultured alone or with *Darc* K/D Mφ, CD82 endocytosis was significantly increased, which was reversed by treatment with recombinant human DARC (rhDARC) or MG-132 (Figures 6J and S6K).

For further validation of our hypothesis, we measured surface CD82 expression of qEML by FACS without removing surface-bound antibodies. As expected, the surface level of CD82 decreased when mono-cultured in proliferation conditions but was maintained when co-cultured with Mφ (Figure S6L). Taken together, our IF and FACS data indicate that qEML mono-culture in proliferation conditions induced CD82 endocytosis and concomitant reduction of surface CD82 expression, which can be blocked by either Mφ DARC or rhDARC. Importantly, while CD82 protein levels fluctuated in reaction to various experimental conditions, *CD82* displayed no significant changes at the mRNA level (Figure S6M).

Although surface CD82 levels had been lowered by ubiquitination-endocytosis in qEML mono-culture, subsequent Mφ co-culture or rhDARC treatment rapidly restored CD82 expression. In contrast, sustained mono-culture or *Darc* K/D Mφ co-culture failed to restore surface CD82 expression (Figures 6K and S6N).

Moreover, as in primary cultures, maintaining qEML cells with *Darc* K/D Raw 264.7 cells resulted in a much lower percentage of qEML cells in G_0. Interestingly, pre-treating qEML cells with rhDARC before co-culture successfully maintained qEML cell dormancy (Figure S6O). Furthermore, rhDARC activated PKCα phosphorylation via interaction with CD82 on qEML cells (Figure S6P).

Thus, 5-FU abolishes DARC-expressing BM Mφ, leading to disruption of the interaction between DARC on Mφ and CD82 on LT-HSCs. This results in ubiquitination, endocytosis, and degradation of CD82 in LT-HSCs. Loss of CD82 causes LT-HSCs to switch to the proliferation/differentiation stage in order to regenerate the BM. After BM regeneration, increased DARC-expressing Mφ recover CD82 expression on LT-HSCs, returning to homeostasis.

The CD82-DARC Interaction Also Maintains Human LT-HSCs

To determine whether CD82 is selectively expressed by and maintains quiescence of primitive HSCs (hereafter HSCs) in humans as well as mice, we examined HSCs from human umbilical cord blood (hUCB). We evaluated CD82 expression on human HSCs ($Lin^-CD34^+CD38^-$ and $Lin^-CD34^-CD38^-CD93^{high}CD45RA^-$) (Anjos-Afonso et al., 2013; Laurenti et al., 2015). CD82 was expressed on ~98% ± 0.5% of $Lin^-CD34^+CD38^-$ cells, a human HSC population with high reconstituting potential (Figure S7A), and on one-quarter of $Lin^-CD34^-CD38^-CD93^{high}CD45RA^-$ HSCs, another quiescent HSC population with severe combined immunodeficiency (SCID)-repopulating capacity at the top of the human hematopoietic hierarchy (Anjos-Afonso et al., 2013) (Figure 7A).

Most $CD82^+$ HSCs were in G_0 phase, while only 20% of $CD82^-$ HSCs were in G_0 (Figure 7B). Additionally, the majority of $CD82^-$ HSCs were positive for Ki-67, a proliferation marker, whereas $CD82^+$ HSCs were primarily Ki-67 negative (Figure 7C). Also, the $CD82^+$ HSC fraction exhibited upregulation of CDK inhibitors (Figure 7C).

To confirm that PKCα phosphorylation is upstream of the CDK inhibitors, $CD82^+$ and $CD82^-$ HSC fractions were treated with rhDARC. PKCα signaling was activated in rhDARC-treated $CD82^+$ HSCs, but not in $CD82^-$ HSCs (Figure 7D). Furthermore, rhDARC blocked G_0 exit of $CD82^+$ HSCs (Figure 7E). As in mice, human monocytes/Mφ exhibited the highest DARC expression level among hUCB component cells. T cells, B cells, Lin^- cells, and ECs exhibited very weak DARC expression (Figure S7B).

To demonstrate DARC functionality in humans, HSPCs (Lin^-DARC^-) were subjected to proliferation conditions and cultured with or without $DARC^+$ monocyte/Mφ or rhDARC. HSCs co-cultured with $DARC^+$ monocyte/Mφ or treated with rhDARC displayed marked upregulation of CD82 (Figure 7F).

In conclusion, CD82 is selectively expressed on primitive HSCs in humans as well; in addition, the majority of $CD82^+$ HSCs are quiescent, which is maintained by DARC-expressing monocytes/Mφ.

DISCUSSION

Our findings, summarized as follows, provide a putative model for quiescence/proliferation cycle of LT-HSCs during

Figure 5. Mφ Express DARC, a Counter-molecule of CD82, and Are Physically Associated with $CD82^+$ LT-HSCs

(A) Representative FACS plot showing surface expression of DARC on BM Mφ ($CD11b^+Gr1^{low}F4/80^+SSC^{low}$).

(B) (Left) $DARC^+F4/80^+$ Mφ in the BM arteriolar niche ($Sca\text{-}1^+$). (Center) High-magnification images of the boxed area in the left figure. Arrows indicate $F4/80^+DARC^+$ Mφ in the arteriolar niche. (Right) Arrows indicate $DARC^+$ Mφ in the BM endosteal niche. Scale bar, 5 μm.

(C) (Top) $CD82^+CD150^+$ LT-HSCs and $DARC^+$ Mφ located adjacent to each other in the BM endosteal and arteriolar niche. Scale bar, 10 μm. (Bottom) $CD82^+Tie2^+$ LT-HSCs and $DARC^+$ Mφ located adjacent to each other in the BM of the Tie2-GFP mouse. Scale bar, 5 μm.

(D) (Top) Schematic representation of the experiment. Lin^- cells, MACS-sorted from the mouse BM, were CFSE-stained and co-cultured with $F4/80^+$ Mφ which were also MACS-sorted from the BM. (Bottom) IF analysis was performed to confirm CD82/DARC interaction. Green- and white-labeled cells are CFSE-stained $CD82^+Lin^-$ cells, and the red cell is an $F4/80^+DARC^+$ macrophage. Scale bar, 10 μm.

(E) CD82/DARC interaction in EML cells was confirmed by co-immunoprecipitation (co-IP).

(F) (Left) Cell-cycle status of the primary LT-HSC gate, which was either mono-cultured or cultured with primary $F4/80^+$ Mφ. (Right) Absolute counts of LT-HSCs in the same set of experiments (**$p < 0.05$, $n = 3$).

(G) (Top) Schematic representation of the experiment. (Center) Cell-cycle status of primary LT-HSCs that were transduced either with mock, *shTgf-b1* or *shSmad3* lentivirus. Mock-transduced HSPCs were either mono-cultured or cultured with primary $F4/80^+$ Mφ, and *shTgf-b1*- and *shSmad3*-transduced HSPCs were cultured with primary $F4/80^+$ Mφ. (Bottom) Phosphorylated Rb expression of LT-HSCs was assessed in the same set of experiment.

All error bars indicate SEM. See also Figure S5.

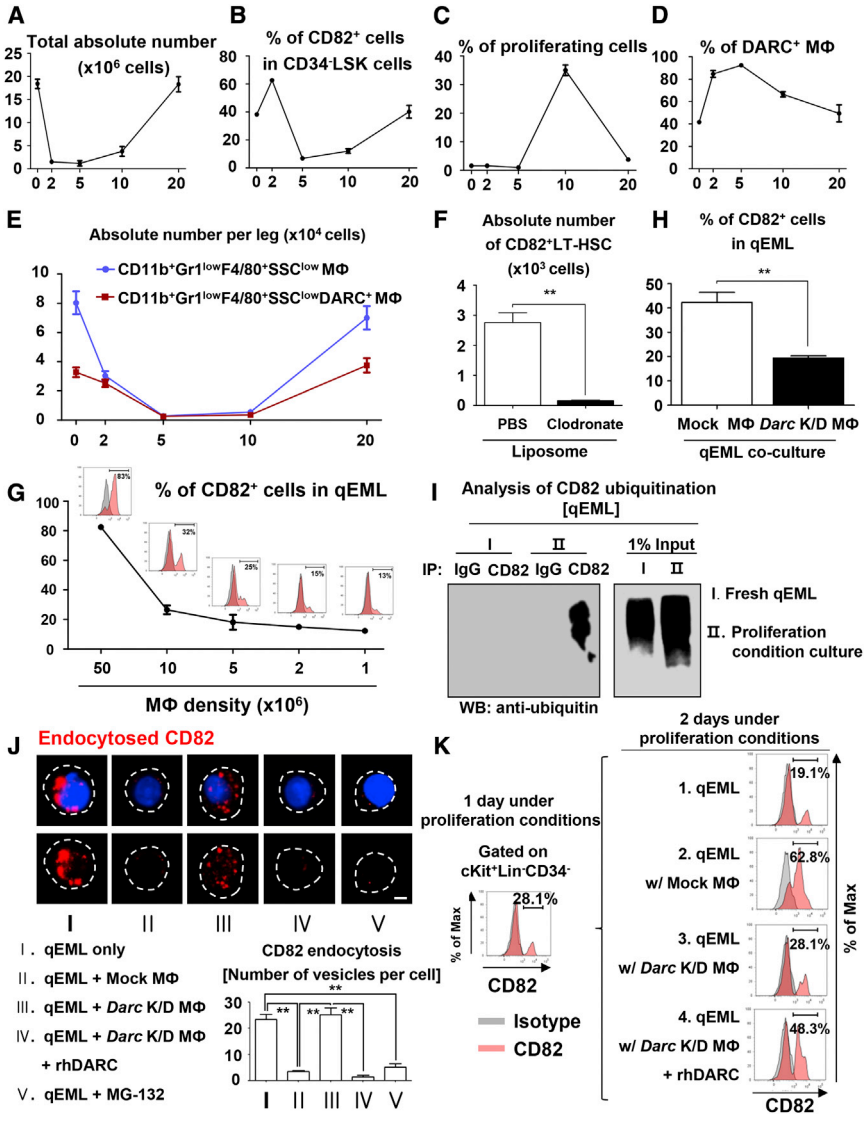

Figure 6. In the BM Niche, DARC-Expressing Mφ Regulate CD82 on LT-HSCs during Homeostasis/Regeneration

(A) Number of total BM cells at different time points after 5-FU injection (n = 6). x axes of Figures 6A–6E represent days after 5-FU injection (day 0). All cell counts in Figure 6 were conducted with BM cells from the femur and tibia of a single hindlimb from WT mice.

(B) Sequential changes in percentage of $CD82^+$ cells in BM LT-HSCs ($CD34^-LSK$) after 5-FU injection (n = 3).

(C) Sequential changes in percentage of proliferating cells (Ki-67^+) in the BM (n = 5).

(D) Sequential changes in percentage of $DARC^{high}$ cells in BM Mφ ($CD11b^+Gr1^{low}F4/80^+SSC^{low}$) after 5-FU injection (n = 3).

(E) Sequential changes in the number of $DARC^{high}$ (red) and total BM Mφ (blue) after 5-FU injection (n = 3). Total Mφ includes the $DARC^{high}$ population. Rapid decrease in $DARC^-$ Mφ in early days after 5-FU treatment led to an increased relative proportion of $DARC^+$ Mφ in the BM.

(F) The number of $CD82^+$ cells in the BM LT-HSC population ($CD34^-Flt3^-LSK$) on the day following treatment with control or clodronate liposomes (**p < 0.05, n = 3).

(G) Changes in $CD82^+$ positivity of qEML cells depending on the density of co-cultured Mφ (n = 3).

(H) Percentage of $CD82^+$ cells in qEML cells that were cultured either with mock or *Darc* K/D Raw 264.7 cells (**p < 0.05, n = 3).

(I) MACS-sorted qEML cells were subjected to proliferation conditions and their protein expression was analyzed by co-IP (CD82) and immunoblot (ubiquitin).

(J) (Top) To analyze CD82 internalization, qEML cells were incubated with biotin-conjugated CD82 antibody and then either mono-cultured (I), cultured with mock Raw 264.7 cells (II), cultured with *Darc* K/D Raw 264.7 cells (III) or cultured with *Darc* K/D Raw 264.7 cells in the presence of rhDARC (IV) or MG-132 (V). After removal of uninternalized antibodies with acid wash, cells were fixed, permeabilized, stained with a fluorescent streptavidin conjugate, and observed using confocal microscopy. (Bottom) CD82 endocytosis was quantified in terms of the number of vesicles per cell (**p < 0.05, n = 5).

(K) Percentage of $CD82^+$ cells (in the c-$Kit^+Lin^-CD34^-$ gate) was measured (left) after 1-day mono-culture of qEML cells. (Right) Later, the cells were further subjected to mono-culture (1), co-culture with mock Mφ (2), co-culture with *Darc* K/D Mφ (3), or co-culture with *Darc* K/D Mφ after 1-hr pretreatment with rhDARC. Two days later, surface CD82 levels were estimated by FACS.

All error bars indicate SEM. See also Figure S6.

the post-ablation recovery process. (1) During homeostasis, CD82 maintains the dormancy of LT-HSCs through interaction with DARC on Mφ. (2) Under BM ablation, $CD82^+$ LT-HSCs and $DARC^+$ Mφ initially resist the ablative stimuli. Then, the $DARC^+$ Mφ population decreases, causing LT-HSCs to lose surface CD82. (3) CD82 loss causes quiescent LT-HSCs to enter the cell cycle and undergo differentiation, regenerating the BM. (4) Newly generated DARC-expressing Mφ brings reduced CD82 expression on LT-HSCs to normal levels and induces cell-cycle exit in LT-HSCs, returning to homeostasis. We also demonstrated CD82/DARC interaction in humans. These findings demonstrate that CD82 is a functional surface marker of LT-HSCs and that the molecule maintains LT-HSC quiescence by interactions with DARC-expressing Mφ.

Until now, several defined sets of surface markers have been used to define higher level BM stem cells, such as LT-HSCs and HSC-1, or quiescent HSCs ($CD150^+CD48^-CD229^-CD244^-LSK$) based on SLAM family markers (Adolfsson et al., 2005; Kiel et al., 2005; Oguro et al., 2013). However, the functions of these markers remain unknown. In this paper, we report that CD82 is a marker for LT-HSCs and has a physiological function in maintaining HSC quiescence, which determines BM reconstituting capability. Our data show that at the mRNA level, *CD82* is expressed predominantly on LT-HSCs while little is detected on ST-HSCs and MPPs. Similar results were observed at the protein

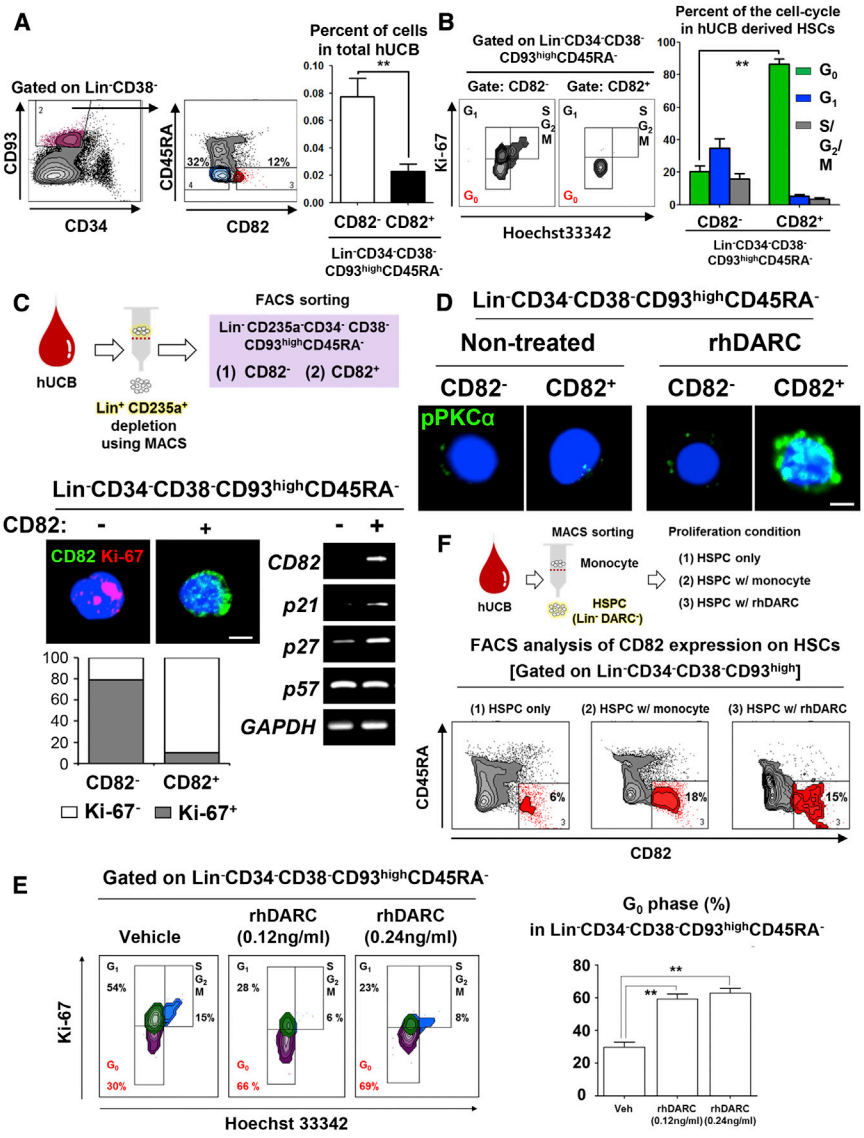

Figure 7. Quiescence of Human CD82$^+$ Primitive HSCs Is Maintained by rhDARC and DARC-Expressing Mφ

(A) (Left) CD82 expression of hUCB-derived primitive HSCs (HSCs, Lin$^-$CD34$^-$CD38$^-$CD93^{high} CD45RA$^-$). (Right) Percentage of CD82$^-$ and CD82$^+$ populations in HSCs (**$p < 0.05$, $n = 4$).

(B) (Left) Cell-cycle status of CD82$^-$ and CD82$^+$ HSCs. (Right) Quantification of the left plot (**$p < 0.05$, $n = 3$).

(C) (Top) Schematic figure showing purification of HSCs. MACS-sorted Lin$^-$CD235a$^-$ hUCB cells were further sorted into two groups (CD34$^-$ CD38$^-$CD93^{high}CD45RA$^-$CD82$^-$ and CD34$^-$ CD38$^-$CD93^{high}CD45RA$^-$CD82$^+$ populations) by FACS. (Bottom left) Representative IF images showing Ki-67 expression in CD82$^-$ and CD82$^+$ HSCs. Quantification of the IF analysis. Scale bar, 2 μm. (Bottom right) mRNA expression of *CD82* and CDK inhibitors (*p21*, *p27*, and *p57*) in CD82$^-$ and CD82$^+$ HSCs.

(D) CD82$^+$ and CD82$^-$ HSCs were separated by FACS, and rhDARC-induced PKCα phosphorylation (pPKCα) was observed by confocal imaging. Scale bar, 2 μm.

(E) (Left) FACS analysis revealed rhDARC blocked G_0 exit of HSCs. (Right) Quantification of the left plot (**$p < 0.05$, $n = 4$).

(F) (Top) Schematic figure of the experiment. Lin$^-$DARC$^-$ HSPCs and monocytes were isolated from hUCB. Lin$^-$DARC$^-$ cells were then cultured alone, co-cultured with monocytes, or treated with rhDARC. (Bottom) CD82 surface expression of the three groups of HSCs (gated on Lin$^-$ CD34$^-$CD38$^-$CD93^{high}) was estimated with FACS. All error bars indicate SEM. See also Figure S7 and Table S3.

level, with larger differences in expression between LT-HSCs and HSPC populations. The significance of this study is that CD82 not only serves as a marker for LT-HSCs but also functions to maintain LT-HSC quiescence. In this regard, it is interesting that the percentage of CD82$^+$ cells in the LT-HSC population (CD34$^-$LSK) increased during the first 2 days after 5-FU challenge (Figure 6B). This implies that CD82$^+$ LT-HSCs are resistant to myeloablation, which might be explained by a comparatively lower proliferation rate (i.e., quiescence) of CD82$^+$ cells.

Our results regarding the mRNA expression pattern of *Cd82* in HSPCs are consistent with those from established databases (http://www.immgen.org and http://gexc.stanford.edu). Although the former shows a different result when the SLAM definition (instead of the Flt3, CD34, and LSK marker combination) is applied, *Cd82* mRNA levels do not necessarily correlate with protein levels. In this study, we showed that there was a significantly higher expression of CD82 in LT-HSC than on either ST-HSC or MPP both at the mRNA and protein levels. Furthermore, considering that CD82 is primarily regulated at the protein level in response to external stimuli (e.g., Mφ co-culture, rhDARC treatment), the analysis of protein levels seems to be a more reliable and accurate indicator of functional expression.

Compared to their WT counterparts, *Cd82*$^{-/-}$ mice had fewer LT-HSCs (Figures 2A–2C) and more myeloid cells (Figure S4F), which implies that *Cd82*$^{-/-}$ LT-HSCs might have undergone myeloid-biased differentiation. This was also demonstrated in our in vivo transplantation model which showed that HSPCs from *Cd82*$^{-/-}$ mice had reduced long-term repopulating capacity and showed myeloid-biased differentiation (Figure 4E), a unique characteristics of aging HSCs (Rossi et al., 2005, 2008). Therefore, we speculate that CD82 regulates the repopulating capacity, aging and lymphoid-myeloid lineage commitment of HSCs.

Because we used whole-body *Cd82* knockout mice, we cannot exclude the possibility that *Cd82* deletion of NSPs may directly or indirectly influence CD82 surface expression or LT-HSC functionality. A series of cell-cycle analyses provide an explanation for CD82 involvement in the LT-HSC and NSP influence on cell-cycle entry and progression of LT-HSCs: after the absence of CD82 on quiescent LT-HSCs allows cells to exit from G_0 and enter G_1 phase, *Cd82* deficiency in LepR$^+$

MSCs accelerates the G_1-to-S/G_2/M transition in LT-HSCs (Figure S7C).

Recent studies have also investigated whether monocytes/Mφ regulate the quiescence or mobilization of HSPCs in a paracrine manner using BM NSPs (Chow et al., 2011; Ehninger and Trumpp, 2011). Importantly, COX-2-induced production in and secretion of PGE_2 from a rare αSMA$^+$ BM Mφ population prevents ROS production in LT-HSCs, thereby maintaining undifferentiated LT-HSCs (Ludin et al., 2012). We found that DARC$^+$ Mφ displayed much higher αSMA and COX-2 expression than the DARC$^-$ fraction (Figures S5D and S5E). Given that after Mφ lose COX-2 activity, they no longer maintain LT-HSC quiescence, there is a possibility that crosstalk exists between the DARC/CD82 axis and COX-2-mediated PGE_2 generation. Our study adds to the findings of Ludin et al. and highlights the importance of Mφ as a HSC niche component governing HSC quiescence.

Most interestingly, HSC-derived megakaryocytes also directly regulate quiescence of HSCs in the BM niche (Bruns et al., 2014; Zhao et al., 2014). We speculate that LT-HSCs themselves differentiate into DARC$^+$ Mφ to regenerate the HSC niche that induces and maintains LT-HSC quiescence. Further studies that employ transgenic mice allowing specific labeling and tracing of DARC will provide more conclusive explanations of the late-stage BM regeneration process.

Generally, the lysosomal degradation axis consists of two branched pathways: endosomes (endolysosomal degradation) or autophagosomes (autophagy). p62 (SQSTM1) is a well-known ubiquitin-binding protein, which is required for the selective autophagy process (Moscat and Diaz-Meco, 2009). Moreover, p62 in osteoblasts can inhibit NF-κB signaling in an endosteal macrophage-dependent manner, which is important for retention of ST-HSCs and hematopoietic progenitors (HPs) (Chang et al., 2014). However, Chang et al. focused only on ST-HSCs and HPs via indirect effects of Mφ. Here, we report that DARC$^+$ Mφ directly regulate LT-HSC retention. DARC$^+$ Mφ, but not DARC$^-$ Mφ, maintained LT-HSC quiescence by physically binding CD82 on the surface of LT-HSCs, thereby preventing its degradation. Further study is required to elucidate whether and how p62 is involved in CD82 degradation, as well as DARC downstream signaling as part of a Mφ-specific mechanism regulating LT-HSC egression.

Our data show little surface expression of DARC on NSPs (e.g., ECs, MSCs and osteoblasts) (Figures S5A and S5C). While human ECs are known to express DARC (Bandyopadhyay et al., 2006), our flow cytometry data clearly show that murine ECs derived from various organs as well as the BM only weakly express DARC (Figures S5A, S5J, and S5K). While endothelial DARC was also shown to regulate LT-HSC quiescence, potential endothelial influence on LT-HSC cell-cycle status through the CD82/DARC axis is unlikely considering the very low level of DARC expression on BM ECs, which highlights the significance of DARC$^+$ Mφ in maintaining HSC quiescence.

In humans as well, rhDARC maintained CD82 expression on HSCs and blocked G_0 exit of HSCs (Figures 7E and 7F). The rhDARC protein we used in this study is embedded in the liposomal membrane, which allows the molecule to fold into and maintain its native 3D structure, thereby exerting its expected functions. Previous reports have shown that DARC also binds both C-C and C-X-C chemokines (Khanna et al., 2014). Thus, the identification of the paracrine factors that mediate the paracrine interaction between DARC$^+$ Mφ and CD82$^+$ HSCs is an important issue for further studies.

Ex vivo expansion of and gene therapy using HSCs are attractive therapeutic strategies for many hematologic diseases in the clinic. Generally, ex vivo expanded HSPCs are actively cycling and have impaired capacity for homing and engraftment compared with freshly isolated HSPCs. While transplantation of ex vivo expanded HSCs in mice showed successful long-term repopulation in many studies, the results were not reproduced in a primate study (Watts et al., 2011).

In human, the majority of Lin$^-$CD34$^+$CD38$^-$ and Lin$^-$CD34$^-$CD38$^-$CD93^{high} HSCs (CD34$^+$ and CD34$^-$ HSCs, respectively) are quiescent and both express significant CD82 levels, which suggests that CD82 may play a role in maintaining quiescence of CD34$^+$ HSCs as well. It is not clear if CD34$^+$ or CD34$^-$ HSCs are more primitive (Engelhardt et al., 2002). Therefore, determining a hierarchical relationship between CD34$^+$CD82$^+$ and CD34$^-$CD82$^+$ cells by estimating the long-term repopulating capacity of the two populations will help resolve this controversy. Also, considering that macrophagic DARC or rhDARC increases surface CD82 expression and induces cell-cycle exit in human CD34$^-$ HSCs, rhDARC treatment may secure the HSC (either CD34$^+$ or CD34$^-$) pool size after BM regeneration by upregulating/restoring surface levels of CD82 on HSCs, forcing them back to dormancy.

One possible therapeutic scheme would be to incubate HSCs with soluble DARC at a specific time point during ex vivo expansion for BMT. Further study is necessary in order to determine the effect of soluble DARC protein on the repopulation capacity of HSCs. Identifying other factors regulating CD82 expression in HSCs and elucidating DARC downstream will facilitate the development and optimization of a treatment protocol capable of exploiting the CD82/DARC axis.

EXPERIMENTAL PROCEDURES

Generation of *Cd82*$^{-/-}$ Mice

To create a conditional targeting vector in which exon 5 and exon 6 of the Cd82 gene were flanked by *loxP* sites, the genomic region from exon 4 to exon 7 used to construct the targeting vector was first subcloned from a BAC clone (Source BioScience) into a pBluescript phagemid system. The FRT-flanked neomycin cassette containing a *loxP* sequence was inserted at the 3′ end of exon 6, and a single *loxP* site was inserted at the 5′ of exon 5. 20 μg targeting vector was linearized using NotI restriction enzyme and transfected into E14Tg2A ES cells (BayGenomics) by electroporation. After neomycin selection, surviving clones were expanded to identify recombinant embryonic stem cell (ESC) clones by Southern blot analysis. Following EcoRI digestion, the bands representing WT and targeted alleles are 11.5 kb and 7.7 kb, respectively. The DNA probe used in Southern blot analysis was a short fragment contained in exon 4. Targeted ESCs were microinjected into C57BL/6 blastocysts, which were used to generate chimeras. Male chimeras were mated to C57BL/6 female mice to obtain F1 heterozygous offspring. The neomycin selection cassette was deleted by crossing targeted heterozygous F1 with FLP deleter mice (The Jackson Laboratory, strain 003946). Genotypes were verified by PCR and Southern blot. The PCR primers used in genotyping were as follows: primer A, 5′-GGGTCCCCTAGGAAATTCAA-3′; primer B, 5′-ATGATGCAGATGTTCTCT CAGGGTG-3′; and primer C, 5′-ACAGGGGACTCACCC TACAAGG-3′.

All mice were backcrossed to C57BL/6 for at least ten generations. Prm-cre transgenic mice were purchased from Taconic. This study was reviewed and approved by the institutional animal care and use committee of the National Cancer Center Research Institute.

Preparation of Human Umbilical Cord Blood Cells

Human umbilical cord blood was collected as follows. After delivery, the cord was clamped and cord blood was collected in a closed system from the umbilical vein using a heparin-coated syringe. Donors were informed with consent guidelines provided by the institutional review board of Seoul National University Hospital (IRB number: H-1210-032-430). After collection, mononuclear cells were obtained using Ficoll-Paque Plus (GE Healthcare Life Sciences) as previously described with slight modifications (Hur et al., 2004). Isolated cells were maintained in "proliferation conditions" (StemSpan H3000, STEMCELL Technologies) media with a cocktail of growth-stimulating cytokines comprising FLT3L, SCF, IL3, and TPO (all from Peprotech).

ACCESSION NUMBERS

The accession number for the RNA-seq data reported in this paper is GEO: GSE56867.

SUPPLEMENTAL INFORMATION

Supplemental Information includes Supplemental Experimental Procedures, seven figures, three tables, and one data (zip) file and can be found with this article online at http://dx.doi.org/10.1016/j.stem.2016.01.013.

AUTHOR CONTRIBUTIONS

J.H., J.-I.C., and Hwan Lee were involved in project planning, experimental work, data analysis, and manuscript preparation; P.N., T.-W.K., C.-W.C., J.-Y.Y., J.-A.K., J.K., S.E.L., C.-H.Y., K.B., and S.H. performed experiments, project planning, and data analysis; T.-Y.R., J.K.J., and Ho Lee discussed and refined the manuscript; and S.H.B and H.-S.K. supervised the project and were involved in project planning, data analysis, and manuscript preparation.

ACKNOWLEDGMENTS

H.-S.K. is supported by the Bio and Medical Technology Development Program of the National Research Foundation (NRF) funded by the Korean government (MSIP) (NRF-2015M3A9B4051041). H.-S.K. is also supported by the Innovative Research Institute for Cell Therapy (A062260) and Korea Health Technology R&D Project (HI14C1277) through the Korea Health Industry Development Institute (KHIDI) funded by the Ministry of Health and Welfare (MHW). J.H. is supported by the Bio and Medical Technology Development Program of the NRF funded by the MSIP (NRF-2015M3A9B4051198). S.H.B. is supported by a grant from the Creative Research Initiatives Program (2009-0081563) of the NRF. The authors would like to thank Prof. Je-Yeol Cho for kindly providing the C166 cell line.

Received: July 8, 2015
Revised: December 10, 2015
Accepted: January 20, 2016
Published: March 17, 2016

REFERENCES

Adams, G.B., and Scadden, D.T. (2006). The hematopoietic stem cell in its place. Nat. Immunol. *7*, 333–337.

Adolfsson, J., Månsson, R., Buza-Vidas, N., Hultquist, A., Liuba, K., Jensen, C.T., Bryder, D., Yang, L., Borge, O.J., Thoren, L.A., et al. (2005). Identification of Flt3+ lympho-myeloid stem cells lacking erythro-megakaryocytic potential a revised road map for adult blood lineage commitment. Cell *121*, 295–306.

Anjos-Afonso, F., Currie, E., Palmer, H.G., Foster, K.E., Taussig, D.C., and Bonnet, D. (2013). CD34(-) cells at the apex of the human hematopoietic stem cell hierarchy have distinctive cellular and molecular signatures. Cell Stem Cell *13*, 161–174.

Arai, F., Hirao, A., Ohmura, M., Sato, H., Matsuoka, S., Takubo, K., Ito, K., Koh, G.Y., and Suda, T. (2004). Tie2/angiopoietin-1 signaling regulates hematopoietic stem cell quiescence in the bone marrow niche. Cell *118*, 149–161.

Bandyopadhyay, S., Zhan, R., Chaudhuri, A., Watabe, M., Pai, S.K., Hirota, S., Hosobe, S., Tsukada, T., Miura, K., Takano, Y., et al. (2006). Interaction of KAI1 on tumor cells with DARC on vascular endothelium leads to metastasis suppression. Nat. Med. *12*, 933–938.

Brenet, F., Kermani, P., Spektor, R., Rafii, S., and Scandura, J.M. (2013). TGFβ restores hematopoietic homeostasis after myelosuppressive chemotherapy. J. Exp. Med. *210*, 623–639.

Bruns, I., Lucas, D., Pinho, S., Ahmed, J., Lambert, M.P., Kunisaki, Y., Scheiermann, C., Schiff, L., Poncz, M., Bergman, A., and Frenette, P.S. (2014). Megakaryocytes regulate hematopoietic stem cell quiescence through CXCL4 secretion. Nat. Med. *20*, 1315–1320.

Chang, K.H., Sengupta, A., Nayak, R.C., Duran, A., Lee, S.J., Pratt, R.G., Wellendorf, A.M., Hill, S.E., Watkins, M., Gonzalez-Nieto, D., et al. (2014). p62 is required for stem cell/progenitor retention through inhibition of IKK/NF-κB/Ccl4 signaling at the bone marrow macrophage-osteoblast niche. Cell Rep. *9*, 2084–2097.

Chow, A., Lucas, D., Hidalgo, A., Méndez-Ferrer, S., Hashimoto, D., Scheiermann, C., Battista, M., Leboeuf, M., Prophete, C., van Rooijen, N., et al. (2011). Bone marrow CD169+ macrophages promote the retention of hematopoietic stem and progenitor cells in the mesenchymal stem cell niche. J. Exp. Med. *208*, 261–271.

Doulatov, S., Notta, F., Laurenti, E., and Dick, J.E. (2012). Hematopoiesis: a human perspective. Cell Stem Cell *10*, 120–136.

Ehninger, A., and Trumpp, A. (2011). The bone marrow stem cell niche grows up: mesenchymal stem cells and macrophages move in. J. Exp. Med. *208*, 421–428.

Engelhardt, M., Lübbert, M., and Guo, Y. (2002). CD34(+) or CD34(-): which is the more primitive? Leukemia *16*, 1603–1608.

Grewal, J.S., Mukhin, Y.V., Garnovskaya, M.N., Raymond, J.R., and Greene, E.L. (1999). Serotonin 5-HT2A receptor induces TGF-beta1 expression in mesangial cells via ERK: proliferative and fibrotic signals. Am. J. Physiol. *276*, F922–F930.

Hur, J., Yoon, C.H., Kim, H.S., Choi, J.H., Kang, H.J., Hwang, K.K., Oh, B.H., Lee, M.M., and Park, Y.B. (2004). Characterization of two types of endothelial progenitor cells and their different contributions to neovasculogenesis. Arterioscler. Thromb. Vasc. Biol. *24*, 288–293.

Khanna, P., Chung, C.Y., Neves, R.I., Robertson, G.P., and Dong, C. (2014). CD82/KAI expression prevents IL-8-mediated endothelial gap formation in late-stage melanomas. Oncogene *33*, 2898–2908.

Kiel, M.J., and Morrison, S.J. (2008). Uncertainty in the niches that maintain haematopoietic stem cells. Nat. Rev. Immunol. *8*, 290–301.

Kiel, M.J., Yilmaz, O.H., Iwashita, T., Yilmaz, O.H., Terhorst, C., and Morrison, S.J. (2005). SLAM family receptors distinguish hematopoietic stem and progenitor cells and reveal endothelial niches for stem cells. Cell *121*, 1109–1121.

Kim, J.H., Kim, B., Cai, L., Choi, H.J., Ohgi, K.A., Tran, C., Chen, C., Chung, C.H., Huber, O., Rose, D.W., et al. (2005). Transcriptional regulation of a metastasis suppressor gene by Tip60 and beta-catenin complexes. Nature *434*, 921–926.

Kim, B., Boo, K., Lee, J.S., Kim, K.I., Kim, W.H., Cho, H.J., Park, Y.B., Kim, H.S., and Baek, S.H. (2010). Identification of the KAI1 metastasis suppressor gene as a hypoxia target gene. Biochem. Biophys. Res. Commun. *393*, 179–184.

Konieczny, S.F., and Emerson, C.P., Jr. (1984). 5-Azacytidine induction of stable mesodermal stem cell lineages from 10T1/2 cells: evidence for regulatory genes controlling determination. Cell *38*, 791–800.

Laurenti, E., Frelin, C., Xie, S., Ferrari, R., Dunant, C.F., Zandi, S., Neumann, A., Plumb, I., Doulatov, S., Chen, J., et al. (2015). CDK6 levels regulate quiescence exit in human hematopoietic stem cells. Cell Stem Cell *16*, 302–313.

Li, C.Y., Suardet, L., and Little, J.B. (1995). Potential role of WAF1/Cip1/p21 as a mediator of TGF-beta cytoinhibitory effect. J. Biol. Chem. *270*, 4971–4974.

Liu, W.M., and Zhang, X.A. (2006). KAI1/CD82, a tumor metastasis suppressor. Cancer Lett. *240*, 183–194.

Ludin, A., Itkin, T., Gur-Cohen, S., Mildner, A., Shezen, E., Golan, K., Kollet, O., Kalinkovich, A., Porat, Z., D'Uva, G., et al. (2012). Monocytes-macrophages

that express α-smooth muscle actin preserve primitive hematopoietic cells in the bone marrow. Nat. Immunol. *13*, 1072–1082.

Miranti, C.K. (2009). Controlling cell surface dynamics and signaling: how CD82/KAI1 suppresses metastasis. Cell. Signal. *21*, 196–211.

Morrison, S.J., and Scadden, D.T. (2014). The bone marrow niche for haematopoietic stem cells. Nature *505*, 327–334.

Moscat, J., and Diaz-Meco, M.T. (2009). p62 at the crossroads of autophagy, apoptosis, and cancer. Cell *137*, 1001–1004.

Oguro, H., Ding, L., and Morrison, S.J. (2013). SLAM family markers resolve functionally distinct subpopulations of hematopoietic stem cells and multipotent progenitors. Cell Stem Cell *13*, 102–116.

Peiper, S.C., Wang, Z.X., Neote, K., Martin, A.W., Showell, H.J., Conklyn, M.J., Ogborne, K., Hadley, T.J., Lu, Z.H., Hesselgesser, J., and Horuk, R. (1995). The Duffy antigen/receptor for chemokines (DARC) is expressed in endothelial cells of Duffy negative individuals who lack the erythrocyte receptor. J. Exp. Med. *181*, 1311–1317.

Petersen, C.P., Weis, V.G., Nam, K.T., Sousa, J.F., Fingleton, B., and Goldenring, J.R. (2014). Macrophages promote progression of spasmolytic polypeptide-expressing metaplasia after acute loss of parietal cells. Gastroenterology *146*, 1727–1738.

Rossi, D.J., Bryder, D., Zahn, J.M., Ahlenius, H., Sonu, R., Wagers, A.J., and Weissman, I.L. (2005). Cell intrinsic alterations underlie hematopoietic stem cell aging. Proc. Natl. Acad. Sci. USA *102*, 9194–9199.

Rossi, D.J., Jamieson, C.H., and Weissman, I.L. (2008). Stems cells and the pathways to aging and cancer. Cell *132*, 681–696.

Scandura, J.M., Boccuni, P., Massagué, J., and Nimer, S.D. (2004). Transforming growth factor beta-induced cell cycle arrest of human hematopoietic cells requires p57KIP2 up-regulation. Proc. Natl. Acad. Sci. USA *101*, 15231–15236.

Shen, Z.J., Esnault, S., Rosenthal, L.A., Szakaly, R.J., Sorkness, R.L., Westmark, P.R., Sandor, M., and Malter, J.S. (2008). Pin1 regulates TGF-beta1 production by activated human and murine eosinophils and contributes to allergic lung fibrosis. J. Clin. Invest. *118*, 479–490.

Silberstein, L.E., and Lin, C.P. (2013). A new image of the hematopoietic stem cell vascular niche. Cell Stem Cell *13*, 514–516.

Takubo, K., Goda, N., Yamada, W., Iriuchishima, H., Ikeda, E., Kubota, Y., Shima, H., Johnson, R.S., Hirao, A., Suematsu, M., and Suda, T. (2010). Regulation of the HIF-1alpha level is essential for hematopoietic stem cells. Cell Stem Cell *7*, 391–402.

Tesio, M., and Trumpp, A. (2011). Breaking the cell cycle of HSCs by p57 and friends. Cell Stem Cell *9*, 187–192.

Tsai, Y.C., Mendoza, A., Mariano, J.M., Zhou, M., Kostova, Z., Chen, B., Veenstra, T., Hewitt, S.M., Helman, L.J., Khanna, C., and Weissman, A.M. (2007). The ubiquitin ligase gp78 promotes sarcoma metastasis by targeting KAI1 for degradation. Nat. Med. *13*, 1504–1509.

Watts, K.L., Adair, J., and Kiem, H.P. (2011). Hematopoietic stem cell expansion and gene therapy. Cytotherapy *13*, 1164–1171.

Winkler, I.G., Barbier, V., Nowlan, B., Jacobsen, R.N., Forristal, C.E., Patton, J.T., Magnani, J.L., and Lévesque, J.P. (2012). Vascular niche E-selectin regulates hematopoietic stem cell dormancy, self renewal and chemoresistance. Nat. Med. *18*, 1651–1657.

Xu, C., Zhang, Y.H., Thangavel, M., Richardson, M.M., Liu, L., Zhou, B., Zheng, Y., Ostrom, R.S., and Zhang, X.A. (2009). CD82 endocytosis and cholesterol-dependent reorganization of tetraspanin webs and lipid rafts. FASEB J. *23*, 3273–3288.

Ye, Z.J., Kluger, Y., Lian, Z., and Weissman, S.M. (2005). Two types of precursor cells in a multipotential hematopoietic cell line. Proc. Natl. Acad. Sci. USA *102*, 18461–18466.

Zhao, M., Perry, J.M., Marshall, H., Venkatraman, A., Qian, P., He, X.C., Ahamed, J., and Li, L. (2014). Megakaryocytes maintain homeostatic quiescence and promote post-injury regeneration of hematopoietic stem cells. Nat. Med. *20*, 1321–1326.

Zon, L.I. (2008). Intrinsic and extrinsic control of haematopoietic stem-cell self-renewal. Nature *453*, 306–313.

Zou, P., Yoshihara, H., Hosokawa, K., Tai, I., Shinmyozu, K., Tsukahara, F., Maru, Y., Nakayama, K., Nakayama, K.I., and Suda, T. (2011). p57(Kip2) and p27(Kip1) cooperate to maintain hematopoietic stem cell quiescence through interactions with Hsc70. Cell Stem Cell *9*, 247–261.